This is a repository copy of *Initiation and Propagation of Transverse Cracking in Composite Laminates*.

Article:

Initiation and Propagation of Transverse Cracking in Composite Laminates

Jianqiao Ye[1]*, Dennis Lam[1] and Daxu Zhang[2]

[1]Institute for Resilient Infrastructure (*i*RI), School of Civil Engineering, University of Leeds, Leeds, LS2 9JT, UK
[2]School of Mechanical, Aerospace and Civil Engineering, University of Manchester, PO Box 88, Manchester, M60 1QD, UK.

Abstract

The matrix cracking transverse to loading direction is usually the one of most common observations of damages in composite laminates. The initiation and propagation of transverse cracks have been a longstanding issue in the last few decades. In this paper, a three-dimensional stress analysis method based on the state space approach is used to compute the stresses, including the inter-laminar stresses near transverse cracks in laminated composites. The stress field is then used to estimate the energy release rate, from which the initiation and propagation of transverse cracking are predicted. The proposed method is illustrated by numerical solutions and is validated by available experimental results. To the best knowledge of the authors, the predictions of crack behaviour for non-symmetrical laminates and laminates subject to in-plane shearing are presented for the first time in the literature.

Introduction

The first form of damages in laminates is usually matrix microcracks. The most common observation of microcracking is cracking in 90º plies during axial loading in the 0º directions (Narin, 2000). Transverse cracking is therefore the most common damage mode in composite materials. An immediate effect of transverse cracking is to cause stiffness degradations of the laminate. Stress singularities near the crack tips at the ply interface may initiate interlaminar delamination. Delamination is not necessarily the ultimate structural failure, but it may result in fibre-matrix debonding and fibre rupture, which will eventually lead to the loss of structural integrity. The

---

*Corresponding author: E-mail: j.ye@leeds.ac.uk,

ultimate failure of a composite laminate follows the occurrence of transverse cracking, longitudinal cracking, delamination and fibre breaking.

The initiation and propagation of transverse cracks in composite laminates have been the focus of failure investigation in the last few decades. Extensive investigations have been carried out both experimentally and analytically.

Garrett and Bailey (1977), Parvizi et al. (1978) and Bailey and Parvizi (1981) are amongst the earliest researchers who carried out extensive experiments to observe transverse cracks. They found that cracks formed in a direction parallel to the transverse reinforcement and the thickness of the 90° plies had significant effect on the cracking process. Flaggs and Kural (1982) presented the results of an experimental study confirming that the constrained transverse cracking phenomena observed in the 90° ply of uniaxially loaded $[0°/90°]_s$ composite laminates was also exhibited by the more general $[\theta/90°]_s$ class of composite laminates. Nairn and Hu (1992), Liu and Nairn (1992) and Nairn et al. (1993) carried out a series of experiments on crack density as a function of applied load. For all the laminates tested, the characteristic cracking curve had no cracks until an onset stress was reached. After the initial crack, the crack density typically increases very rapidly. The onset stress decreases as the thickness of the 90° plies increases. Yokozeki et al. (2005) investigated crack accumulation in multiple plies of $[0/\theta_2/90°]_s$ laminates ($\theta=30°$, 45° and 60°). Most of the experimental investigations showed that the first damage mode was usually transverse cracking. Both the thickness of 90° layers and the stiffness of constrain layers affected the initiation and propagation of transverse cracks.

The majority of earlier analytical work on transverse cracking assumed that cracks formed when the stress or strain reached the transverse strength of a ply material. Garrett and Bailey (1977) assumed that a transverse ply had a unique breaking strain, ε_{tu}, and strength σ_{tu}. If a stress is applied in a direction parallel to the longitudinal plies, the transverse ply will fail at a stress σ_{tu}. Using the same strength criteria, Parvizi, et al (1978) reported more detailed studies for a glass fibre reinforced epoxy composite. Leblond et al. (1996) studied multiplication of transverse cracks as a function of applied stress in cross-ply laminates. The crack development was assumed to be controlled by the fracture stress in the 90° plies. However the strength based theory usually can not provide a good prediction of transverse cracking because

the strength of 90° plies of a laminate is usually not the same as that of a different laminate.

Due to the drawbacks and limitations of the strength based methods, the majority of recent work was based fracture mechanics using the energy method to predict transverse cracking. Most energy models used a representative volume element (RVE) to predict next crack formation when the energy released due to crack formation reached the critical strain energy release rate G_c. It has been widely recognised that for the same material ply laminates with different lamination profiles, the value of G_c almost keeps constant (Nairn, 2000). Consequently, the method applies for a wide variety of laminates from a single value of G_c.

Parvizi et al. (1978) demonstrated that a simple shear lag analysis used in conjunction with the Griffith energy criterion can be used to accurately predict matrix cracking. Flaggs (1985) made use of a strain energy release rate fracture criteria in conjunction with an approximate two-dimensional shear-lag model to predict tensile matrix failure. Wang et al (1985) employed the energy release rate method of classical fracture mechanics to model various matrix crack interactions. Dvorak and Laws (1987) investigated the first ply failure using a critical energy release rate criteria and later Laws and Dvorak (1988) presented a model for progressive transverse cracking based on statistical fracture mechanics. Nairn (1989; 2000), Liu and Nairn, (1992) and Nairn and Hu (1992) carried out a series of study on matrix cracking by finite fracture mechanics. Zhang et al. (1992) and Fan and Zhang (1993) proposed the equivalent constraint model (ECM), in which the energy release rate due to transverse ply cracking, incorporating residual thermal stresses, was derived. McCartney (1998; 2002; 2004; 2005) investigated ply crack development for various lamination profiles; from cross-ply to general symmetric laminates, subjected to axial extension or mixed mode loading. Smith and Ogin (1999) calculated the critical bending moment at transverse cracking under flexural loads using a fracture mechanics approach. Joffe et al. (2001) used a crack-closure technique to calculate the energy release caused by cracking. A Monte-Carlo simulation in incremental strain-controlled loading was used to model the transverse cracking process. The 90° layer was divided into a large number of elements and a critical energy release rate G_c was assigned to each element according to Weibull distribution. Yokozeki el al. (2002) employed energy release rate to investigate crack initiation and propagation across specimen width. Energy

release rates associated with crack propagation in the width direction were calculated using a three-dimensional FEA. Subsequently Yokozeki et al. (2005) used the same method to study micro-cracking behaviour induced by matrix cracks in adjacent plies. Lim and Li (2005) calculated energy release rates for transverse cracking and delamination under the generalised plane strain condition. By introducing the minimum strain energy density criterion to a non-linear FE analysis, Sirivedin et al. (2006) predicted matrix crack propagation in continuous-carbon fibre/epoxy composites.

It is obvious that for an energy based method, an accurate prediction of the stress distribution within a RVE is essential to an accurate estimate of the potential energy within the element. This is particularly difficult for a laminated RVE with transverse cracks. Traditional analysis of laminated composites used classic or higher order plate theories that usually provided unsatisfactory predictions to interfacial stresses and the stress singularities at the tips of transverse cracks. Zhang and Ye (2007a) recently developed an analytical model that can provide accurate predictions to the stress fields, including all the interfacial stresses, and a satisfactory approximation to the stress singularities near ply cracks. The model was based on a state space approach that has been successfully used to solve a variety of stress problems (Soldatos and Ye, 1994; Ye and Soldatos, 1994a, b, 1995; Ye and Sheng, 2003; Ye et al., 2004; Zhang and Ye, 2007b). Compared with other analytical models, this new model takes full three-dimensional consideration of laminar properties, displacements and interfacial stress continuities at all material interfaces. The model can also deal with both symmetric and non-symmetric laminates with a universal approach. A comprehensive account of the methodology can be found in Ye (2002).

In combination with the state space formulation (Ye, 2002) this paper presents a model to predict crack propagation by using an energy based approach. An accurate stress distribution within a RVE with cracks is obtained from the state space solution. The stresses are then used to compute the energy release rate in the crack propagation analysis. Numerical results are obtained and compared with the tests results available in the literature. Results are also presented for non-symmetric laminates and laminates subjected to in-plane shearing. From the authors' best knowledge, these results are new and are not available in the literature.

Stresses of angle-ply laminates with transverse cracks

Solution of an angle-ply lamina

Consider an off-axis lamina (Fig. 1) with principal material directions (1-2-3) in the global *x-y-z* coordinate system. The lamina has constant thickness *h*, width *L* and infinite length. The displacements in the *x*, *y* and *z* directions are denoted by *u*, *v* and *w*, respectively. Suppose that the lamina is subjected to a uniform tension by the application of a constant longitudinal strain in the y direction, ε_0 ,which represents a laminate that is long and relatively uniform in one direction, such as aircraft wing panels. The constant strain in the y direction also represents the state of stress at a point in a material subject to a generalized plane strain, where the stresses and strains in other two directions are more dominating.

The lamina is made of a homogeneous, monoclinic and linearly elastic material whose principal material direction 1, i.e., the fiber direction, has an angle of θ to the *x* axis.

(a) Stress-strain relations

The basic constitutive equation for thermo-elastic stress analysis is (Herakovich, 1998)

$$\{\sigma\} = [C](\{\varepsilon\} - \{\varepsilon^T\}) . \tag{1}$$

Here, the matrices $[C]$, $\{\varepsilon\}$ and $\{\varepsilon^T\}$ are stiffness matrix, total strains and thermal strains, respectively. For a linearly elastic monoclinic material,

$$[C] = \begin{bmatrix} C'_{11} & C'_{12} & C'_{13} & 0 & 0 & C'_{16} \\ C'_{12} & C'_{22} & C'_{23} & 0 & 0 & C'_{26} \\ C'_{13} & C'_{23} & C'_{33} & 0 & 0 & C'_{36} \\ 0 & 0 & 0 & C'_{44} & C'_{45} & 0 \\ 0 & 0 & 0 & C'_{45} & C'_{55} & 0 \\ C'_{16} & C'_{26} & C'_{36} & 0 & 0 & C'_{66} \end{bmatrix}, \tag{2}$$

where the C'_{ij} are stiffness coefficients that can be expressed in terms of Young's moduli, Poisson's ratios and shear moduli.

$$\{\varepsilon\} = [\varepsilon_{xx} \quad \varepsilon_{yy} \quad \varepsilon_{zz} \quad \varepsilon_{yz} \quad \varepsilon_{xz} \quad \varepsilon_{xy}]^T , \tag{3}$$

$$\{\varepsilon^T\} = \{\alpha\}\Delta T , \tag{4}$$

where ΔT denotes temperature change,

$$\{\alpha\} = [\alpha_{xx} \quad \alpha_{yy} \quad \alpha_{zz} \quad 0 \quad 0 \quad \alpha_{xy}]^T , \tag{5}$$

where α_{xx}, α_{yy}, α_{zz} and α_{xy} are the coefficients of axial thermal expansion relative to the *x, y, z* directions and shear thermal expansion, respectively.

(b) Equilibrium equations

$$\begin{cases} \dfrac{\partial \sigma_{xx}}{\partial x} + \dfrac{\partial \sigma_{xy}}{\partial y} + \dfrac{\partial \sigma_{xz}}{\partial z} = 0 \\[3mm] \dfrac{\partial \sigma_{xy}}{\partial x} + \dfrac{\partial \sigma_{yy}}{\partial y} + \dfrac{\partial \sigma_{yz}}{\partial z} = 0 \\[3mm] \dfrac{\partial \sigma_{xz}}{\partial x} + \dfrac{\partial \sigma_{yz}}{\partial y} + \dfrac{\partial \sigma_{zz}}{\partial z} = 0 \end{cases} . \tag{6}$$

(c)   Strain-displacement relations

$$\begin{cases} \varepsilon_{xx} = \dfrac{\partial u}{\partial x}, \qquad \varepsilon_{yy} = \dfrac{\partial v}{\partial y}, \qquad \varepsilon_{zz} = \dfrac{\partial w}{\partial z} \\[3mm] \varepsilon_{yz} = \dfrac{\partial w}{\partial y} + \dfrac{\partial v}{\partial z}, \quad \varepsilon_{xz} = \dfrac{\partial u}{\partial z} + \dfrac{\partial w}{\partial x}, \ \varepsilon_{xy} = \dfrac{\partial u}{\partial y} + \dfrac{\partial v}{\partial x} \end{cases} . \tag{7}$$

Since the lamina is subjected to a uniform extension ε_0 in the y direction, it follows that

$$\varepsilon_{yy} = \frac{\partial v}{\partial y} = \varepsilon_0 . \tag{8}$$

Then the generalized plane strain deformation is assumed such that all components of stress and strain do not depend upon y.

To carry out the following deductions, let

$$\alpha = \partial / \partial x , \ C_1 = -C_{13}' / C_{33}' , \ C_2 = C_{11}' - C_{13}'^2 / C_{33}' , \ C_3 = C_{12}' - C_{13}' C_{23}' / C_{33}' ,$$

$$C_4 = C_{22}' - C_{23}'^2 / C_{33}' , \ C_5 = -C_{23}' / C_{33}' , \ C_6 = -C_{36}' / C_{33}' , \ C_7 = 1/C_{33}' , \ C_8 = 1/C_{55}' ,$$

$$C_9 = C_{16}' - C_{13}' C_{36}' / C_{33}' , \ C_{10} = C_{26}' - C_{23}' C_{36}' / C_{33}' , \ C_{11} = C_{45}' / \Delta , \ C_{12} = C_{44}' / \Delta , \ C_{13} = C_{55}' / \Delta ,$$

$$C_{14} = C_{66}' - C_{36}'^2 / C_{33}' , \ \Delta = C_{45}'^2 - C_{44}' C_{55}' . \tag{9}$$

From the third equation of Eq. (1) and Eq. (7), one has

$$\frac{\partial w}{\partial z} = C_1 \alpha u + C_6 \alpha v + C_7 \sigma_{zz} + C_5 \varepsilon_0 - (C_1 \alpha_{xx} + C_5 \alpha_{yy} + C_6 \alpha_{xy} - \alpha_{zz}) \Delta T . \tag{10}$$

By substituting Eq. (7) into the first, second and sixth equations of Eq. (1), the in-plane stresses can be expressed as

$$\begin{Bmatrix} \sigma_{xx} \\ \sigma_{yy} \\ \sigma_{xy} \end{Bmatrix} = \begin{bmatrix} C_2 \alpha & C_9 \alpha & -C_1 \\ C_3 \alpha & C_{10} \alpha & -C_5 \\ C_9 \alpha & C_{14} \alpha & -C_6 \end{bmatrix} \begin{Bmatrix} u \\ v \\ \sigma_{zz} \end{Bmatrix} + \begin{Bmatrix} C_3 \\ C_4 \\ C_{10} \end{Bmatrix} \varepsilon_0 - \begin{Bmatrix} C_2 \alpha_{xx} + C_3 \alpha_{yy} + C_9 \alpha_{xy} \\ C_3 \alpha_{xx} + C_4 \alpha_{yy} + C_{10} \alpha_{xy} \\ C_9 \alpha_{xx} + C_{10} \alpha_{yy} + C_{14} \alpha_{xy} \end{Bmatrix} \Delta T . \tag{11}$$

Inserting Eq. (11) into Eq. (6) and considering Eq. (10) as well as the fourth and fifth equations of Eq. (1), the following first order partial differential equation can be obtained

6

$$\frac{\partial}{\partial z}\begin{Bmatrix} u \\ v \\ w \\ \sigma_{xz} \\ \sigma_{yz} \\ \sigma_{zz} \end{Bmatrix} = \begin{bmatrix} 0 & 0 & -\alpha & -C_{12} & C_{11} & 0 \\ 0 & 0 & 0 & C_{11} & -C_{13} & 0 \\ C_1\alpha & C_6\alpha & 0 & 0 & 0 & C_7 \\ -C_2\alpha^2 & -C_9\alpha^2 & 0 & 0 & 0 & C_1\alpha \\ -C_9\alpha^2 & -C_{14}\alpha^2 & 0 & 0 & 0 & C_6\alpha \\ 0 & 0 & 0 & -\alpha & 0 & 0 \end{bmatrix}\begin{Bmatrix} u \\ v \\ w \\ \sigma_{xz} \\ \sigma_{yz} \\ \sigma_{zz} \end{Bmatrix} + \begin{Bmatrix} 0 \\ 0 \\ C_5\varepsilon_0 - (C_1\alpha_{xx} + C_5\alpha_{yy} + C_6\alpha_{xy} - \alpha_{zz})\Delta T \\ 0 \\ 0 \\ 0 \end{Bmatrix}$$

(12)

Assuming that displacements u, v, and w can be expressed, respectively, as

$$\begin{cases} u(x,y,z) = \bar{u}(x,z) + U^{(0)}(z)\left(1 - \dfrac{2x}{L}\right) \\ v(x,y,z) = \bar{v}(x,z) + V^{(0)}(z)\left(1 - \dfrac{2x}{L}\right) + \varepsilon_0 y, \\ w(x,y,z) = w(x,z) \end{cases}$$

(13)

where $U^{(0)}(z)$ and $V^{(0)}(z)$ are unknown boundary displacements that can be determined by imposing traction free conditions along the stress free surfaces (see the boundary condition section). In Eq.(13), the following Fourier series expansions are assumed

$$\begin{Bmatrix} \bar{u} \\ \bar{v} \\ w \\ \sigma_{xz} \\ \sigma_{yz} \\ \sigma_{zz} \end{Bmatrix} = \sum_{m=0}^{\infty} \begin{Bmatrix} \bar{U}_m(z)\sin(\xi x) \\ \bar{V}_m(z)\sin(\xi x) \\ W_m(z)\cos(\xi x) \\ X_m(z)\sin(\xi x) \\ Y_m(z)\sin(\xi x) \\ Z_m(z)\cos(\xi x) \end{Bmatrix},$$

(14)

where $\xi = m\pi/L$. In the case of a uniform extension in the x-direction, the axial displacement u is zero at $x=L/2$. Hence, the integer m in Eq. (14) and the equations below takes only even numbers, i.e. $m = 0, 2, 4, \ldots$.

By introducing Eqs. (13) and (14) into (12) and expanding the x and 1 in Eq. (13) into also Fourier series, the following non-homogenous state space equation for an arbitrary value of m is obtained

$$\frac{d}{dz}\{\mathbf{F}_m(z)\} = [\mathbf{G}_m]\{\mathbf{F}_m(z)\} + \{\mathbf{B}_m(z)\},$$

(15a)

where

$$\{\mathbf{F}_m(z)\} = [\bar{U}_m(z) \quad \bar{V}_m(z) \quad W_m(z) \quad X_m(z) \quad Y_m(z) \quad Z_m(z)]^{\mathrm{T}},$$

(15b)

7

$$[\mathbf{G}_m] = \begin{bmatrix} 0 & 0 & \xi & -C_{12} & C_{11} & 0 \\ 0 & 0 & 0 & C_{11} & -C_{13} & 0 \\ C_1\xi & C_6\xi & 0 & 0 & 0 & C_7 \\ C_2\xi^2 & C_9\xi^2 & 0 & 0 & 0 & -C_1\xi \\ C_9\xi^2 & C_{14}\xi^2 & 0 & 0 & 0 & -C_6\xi \\ 0 & 0 & 0 & -\xi & 0 & 0 \end{bmatrix}, \tag{15c}$$

$$\{\mathbf{B}_0(z)\} = \left[0,0, C_5\varepsilon_0 - (C_1\alpha_{xx} + C_5\alpha_{yy} + C_6\alpha_{xy} - \alpha_{zz})\Delta T - \frac{2C_1}{L}U^{(0)}(z) - \frac{2C_6}{L}V^{(0)}(z),0,0,0 \right]^T, \tag{15d}$$

$$\{\mathbf{B}_m(z)\} = \left[-\frac{2}{m\pi}(1 + \cos m\pi)\frac{dU^{(0)}(z)}{dz}, -\frac{2}{m\pi}(1 + \cos m\pi)\frac{dV^{(0)}(z)}{dz}, 0,0,0,0 \right]^T \quad (m = 2, 4, 6 \ldots). \tag{15e}$$

The solution of the non-homogenous state space Eq. (15) is

$$\{\mathbf{F}_m(z)\} = e^{[\mathbf{G}_m]z}\{\mathbf{F}_m(0)\} + \int_0^z e^{[\mathbf{G}](z-\tau)}\{\mathbf{B}_m(\tau)\}d\tau$$

$$= [\mathbf{D}_m(z)]\{\mathbf{F}_m(0)\} + \{\mathbf{H}_m(z)\}, z \in [0, h]. \tag{16}$$

In particular, at $z = h$,

$$\{\mathbf{F}_m(h)\} = [\mathbf{D}_m(h)]\{\mathbf{F}_m(0)\} + \{\mathbf{H}_m(h)\}, \tag{17}$$

where $[\mathbf{D}_m(h)]$ is called transfer matrix. The calculation of the two constant matrices, $[\mathbf{D}_m(h)]$ and $\{\mathbf{H}_m(h)\}$, in Eq. (17) can be found either analytically or numerically from Ye (2002).

Solution of an angle-ply laminate

Consider an infinite long multi-layered general angle-ply laminate of thickness H and width L. Again the laminate is subjected to a constant longitudinal strain, ε_0. We may imagine that it is composed of N fictitious sub-layers, each of which may have different thickness. However, it is assumed that the thickness of all the fictitious sub-layers approach zero uniformly as N approaches infinity. Assuming, in addition, that different sub-layers may be composed of different monoclinic materials, two types of materials interfaces are distinguished in the plate; the fictitious interfaces which separate sub-layers with the same material properties and the real ones that separate sub-layers composed of different materials. Upon choosing a suitably large value of N, each individual sub-layer becomes thin. For each of the sub-layers, (15)-(17) are the solutions. The state space equation and the form of solution of an arbitrary sub-

layer, e.g., the jth one whose thickness is h_j, can easily be obtained by replacing h with h_j in Eqs. (15)- (17). The state space equation of the jth sub-layer then becomes:

$$\frac{d}{dz}\{\mathbf{F}_m(z)\}_j = [\mathbf{G}_m]_j \{\mathbf{F}_m(z)\}_j + \{\mathbf{B}_m(z)\}_j .$$ (18)

After repeating the above process for all the individual sub-layers and with appropriate continuity requirements imposed at all the real and fictitious interfaces, a solution for the entire laminate can be formulated.

In order to find the solution of the problem, the two unknown displacement components, $U^{(0)}(z)$ and $V^{(0)}(z)$ in Eq. (15) must be determined first. If the sub-layers of the laminate are all sufficiently thin, it is reasonable to assume that $U^{(0)}(z)$ and $V^{(0)}(z)$ within the thin layer are linearly distributed in the z direction, i.e.

$$\begin{cases} U_j^{(0)}(z) = U_j^-(1-\dfrac{z}{h_j}) + U_j^+ \dfrac{z}{h_j} \\ V_j^{(0)}(z) = V_j^-(1-\dfrac{z}{h_j}) + V_j^+ \dfrac{z}{h_j} \end{cases}, z \in [0, \ h_j], \qquad j=1, 2,\ldots, N,$$ (19)

where U_j^-, U_j^+, V_j^- and V_j^+ are the values of $U_j^{(0)}(z)$ and $V_j^{(0)}(z)$ at the top and bottom surfaces of the jth thin layer, respectively. Inserting Eq. (19) into Eqs. (15d) and (15e), vector $\{\mathbf{B}_m(z)\}_j$ in Eq. (18) can be expressed as

$$\{\mathbf{B}_0(z)\}_j = [0,0, C_5\varepsilon_0 - (C_1\alpha_x + C_5\alpha_y + C_6\alpha_{xy} - \alpha_z)\Delta T$$
$$- \frac{2C_1}{L}\left(U_j^-(1-\frac{z}{h_j}) + U_j^+\frac{z}{h_j}\right) - \frac{2C_6}{L}\left(V_j^-(1-\frac{z}{h_j}) + V_j^+\frac{z}{h_j}\right),0,0,0]^T, \ z \in [0, \ h_j],$$ (20a)

$$\{\mathbf{B}_m(z)\}_j = \left[\frac{4}{m\pi}\frac{U_j^- - U_j^+}{h_j}, \frac{4}{m\pi}\frac{V_j^- - V_j^+}{h_j},0,0,0,0\right]^T \ (m=2, 4, 6\ldots).$$ (20b)

The solution of Eq.(18) at $z=h_j$ is

$$\{\mathbf{F}_m(h_j)\}_j = [\mathbf{D}_m(h_j)]_j \{\mathbf{F}_m(0)\}_j + \{\mathbf{H}_m(h_j)\}_j .$$ (21)

By introducing the following continuity conditions at all interfaces, i.e.,

$$\{\mathbf{F}_m(0)\}_{j+1} = \{\mathbf{F}_m(h_j)\}_j , j=1, 2,\ldots, N\text{-}1,$$ (22)

and then using Eqs.(21) and (22) recursively, a relationship between the state vectors on the top and bottom surfaces of the laminate is established as follows:

$$\{\mathbf{F}_m(h_N)\}_N = [\bar{\mathbf{D}}_m]_N \{\mathbf{F}_m(0)\}_1 + \{\bar{\mathbf{H}}_m\} ,$$ (23a)

where

$$\left[\overline{\mathbf{D}}_m\right]_N = \left(\prod_{j=N}^{1} \left[\mathbf{D}_m(h_j)\right]_j\right),$$ (23b)

$$\left\{\overline{\mathbf{H}}_m\right\} = \left(\prod_{j=N}^{2} \left[\mathbf{D}_m\right]_j\right)\left\{\mathbf{H}_m\right\}_1 + \left(\prod_{j=N}^{3} \left[\mathbf{D}_m\right]_j\right)\left\{\mathbf{H}_m\right\}_2 + \cdots + \left\{\mathbf{H}_m\right\}_N.$$ (23c)

$\{\mathbf{F}_m(h_N)\}_N$ and $\{\mathbf{F}_m(0)\}_1$ are, respectively, the state vectors at the top and bottom surfaces of the laminated composite. The traction free conditions at the top and bottom surfaces yields

$$\begin{cases} \left[X_m(0) \quad Y_m(0) \quad Z_m(0)\right]_1^T = \left[0 \quad 0 \quad 0\right]^T \\ \left[X_m(h_N) \quad Y_m(h_N) \quad Z_m(h_N)\right]_N^T = \left[0 \quad 0 \quad 0\right]^T \end{cases}.$$ (24)

Substituting Eq. (24) into Eq. (23) results in the following linear algebra equation system

$$\begin{bmatrix} \overline{D}_{41} & \overline{D}_{42} & \overline{D}_{43} \\ \overline{D}_{51} & \overline{D}_{52} & \overline{D}_{53} \\ \overline{D}_{61} & \overline{D}_{62} & \overline{D}_{63} \end{bmatrix} \begin{Bmatrix} \overline{U}_m \\ \overline{V}_m \\ \overline{W}_m \end{Bmatrix}_1 = - \begin{Bmatrix} \overline{H}_{m4} \\ \overline{H}_{m5} \\ \overline{H}_{m6} \end{Bmatrix},$$ (25)

where $\overline{D}_{ij}$ and $\overline{H}_{mi}$ are the matrix elements in $\left[\overline{\mathbf{D}}_m\right]$ and $\{\overline{\mathbf{H}}_m\}$ of Eqs.(23b- 23c) that are related to the three displacement components at the bottom surface, respectively.

Eq.(25) is a set of linear algebra equations in terms of the three displacement components, $\overline{U}_m$, $\overline{V}_m$ and W_m, at the top surface. The terms on the right-hand side of Eq. (25), $\overline{H}_{m4}$, $\overline{H}_{m5}$ and $\overline{H}_{m6}$, contain $4 \times N$ unknown constants, U_j^-, U_j^+, V_j^-, and V_j^+ (j=1, 2,…N), introduced in Eq.(19). Because of the continuity of $U^{(0)}(z)$ and $V^{(0)}(z)$ at the interface between the jth and the (j+1)th sub-layers, $U_j^+ = U_{j+1}^-$ and $V_j^+ = V_{j+1}^-$ (j=1, 2,…N-1). Hence, the number of unknown constants is then reduced to 2(N+1). These constants are determined by introducing appropriate boundary conditions along the transverse edges.

Ply-crack boundary conditions

When a general angle-ply laminate is subjected to an in-plane extension perpendicular to the 90° fibers, transverse ply cracks appear parallel to the fibers and across the entire width from edge to edge. For example, subject to a uniform biaxial extension, ε_0 and F_0, and a shear loading, S_0, the [θ°$_m$/90°$_n$/ϕ°$_s$] laminate shown in Fig. 2 displays an array of periodic cracks in the 90°$_n$ layers, where the subscripts

denote the number of the real plies within a ply group. In reality, matrix cracks can occur in any plies, but there are a large group of laminates, in which transverse cracking in 90º plies is the dominated damage mode, and therefore the minor matrix cracking in non-90º plies is ignored in the present model. Other damage modes, e.g. delamination and fibre breakage usually occur at high crack densities, so the current work focuses on low and intermediate crack densities.

Assuming that the cracks are equally spaced, a representative volume element (Fig. 3) can be taken from any two neighboring cracks to predict the stress and displacement fields.

For the cracked layers at $x=0$, L the boundary conditions are traction free, i.e., $\sigma_{xx} = \sigma_{xy} = 0$. For the un-cracked layers at $x=0$, L, due to the fact that the laminate is subjected to uniform extension and shear loading, the displacements of an uncracked layer in the x and y directions, u and v, remain constant, that is

$$\begin{cases} u(0,y,z) = u_0 \\ v(0,y,z) = v_0 \end{cases}.$$

(26a)

Substituting Eq. (26a) and Eq. (14) into Eq. (5.13) yields at x=0 and y=0

$$\begin{cases} u(0,0,z) = \sum_{m=0}^{\infty} \overline{U}_m(z) \sin(\xi \times 0) + U^{(0)}(z)\left(1 - \frac{2 \times 0}{L}\right) = u_0 \\ v(0,0,z) = \sum_{m=0}^{\infty} \overline{V}_m(z) \sin(\xi \times 0) + V^{(0)}(z)\left(1 - \frac{2 \times 0}{L}\right) + \varepsilon_0 \times 0 = v_0 \end{cases}$$

(26b)

From also the equilibrium of the internal and external forces, the following equation exists

$$\begin{cases} \int_h \sigma_{xx} dz = F_0 \\ \int_h \sigma_{xy} dz = S_0 \end{cases}$$

(27a)

or, from Eq.(11)

11

$$\begin{cases} \int_h \left(\sum_m \left[C_2 \xi \overline{U}_m(z) + C_9 \xi \overline{V}_m(z) - C_1 Z_m(z) \right]_j + \left[C_3 \varepsilon_0 - (C_2 \alpha_x + C_3 \alpha_y + C_9 \alpha_{xy}) \Delta T \right]_j \right. \\ \left. - \left[\frac{2C_2}{L} U^{(0)}(z) + \frac{2C_9}{L} V^{(0)}(z) \right]_j \right) dz = F_0 \\ \int_h \left(\sum_m \left[C_9 \xi \overline{U}_m(z) + C_{14} \xi \overline{V}_m(z) - C_6 Z_m(z) \right]_j + \left[C_{10} \varepsilon_0 - (C_9 \alpha_x + C_{10} \alpha_y + C_{14} \alpha_{xy}) \Delta T \right]_j \right. \\ \left. - \left[\frac{2C_9}{L} U^{(0)}(z) + \frac{2C_{14}}{L} V^{(0)}(z) \right]_j \right) dz = S_0 \end{cases}$$

$$(27b)$$

where F_0 and S_0 are the forces per unit length (Fig. 3). From the introduction of the boundary conditions, it can be seen that the solution can be found to the required accuracy by increasing the total number of the thin layers.

Propagation of transverse cracking in laminates

The total complementary potential energy of a representative element

Fig. 3 shows a representative volume element which is taken from between two neighboring cracks in a $[\theta°_m/90°_n/\phi°_s]$ composite laminate. Assuming that stress analysis has been carried out on this idealized element from the previous section, where the laminate was assumed to consist of N fictitious sub-layers. By using the present stress analysis, the total complementary potential energy is easier to obtain than the total potential energy because the stresses, used to calculate the complementary strain energy, are determined immediately after solving the state space equations. The complementary strain energy U_c of this representative element is

$$U_c = \sum_{j=1}^{N} U_c^j \qquad (28)$$

where the superscript 'j' denotes the jth sub-layer and U_c^j is the complementary strain energy of the jth sub-layer of the representative volume element. Using the stresses from the previous section, U_c^j per unit length in the y direction can be obtained as

$$U_c^j = \frac{1}{2} \int_0^{h_j} \int_0^L \left[\{\sigma\}^T [C']^{-1} \{\sigma\} + \Delta T \{\alpha\}^T \{\sigma\} \right]_j dx dz \qquad (29a)$$

where

$$\{\sigma\} = [\sigma_{xx} \quad \sigma_{yy} \quad \sigma_{zz} \quad \sigma_{yz} \quad \sigma_{xz} \quad \sigma_{xy}]^T \qquad (29b)$$

12

Considering that the laminate is under a uniformly prescribed strain ε_0 in the y direction, the potential of the prescribed strain ε_0 can be calculated as

$$V_c = \sum_{j=1}^{N} V_c^{\,j} = \sum_{j=1}^{N} \int_{0}^{h_j} \int_{0}^{L} \left[\varepsilon_0 \sigma_{yy} \right]_j dxdz \qquad (30)$$

The total complementary potential energy of this representative volume element is given as the difference of the complementary strain energy U_c and the potential of prescribed displacements V_c.

$$\Gamma = U_c - V_c = \sum_{j=1}^{N} \int_{0}^{h_j} \int_{0}^{L} \left[\frac{1}{2} \left(\{\sigma\}^T [C']^{-1} \{\sigma\} + \Delta T \{\alpha\}^T \{\sigma\} \right) - \varepsilon_0 \sigma_{yy} \right]_j dxdz \qquad (31)$$

The energy release rate due to transverse cracking

Consider a composite laminate subjected to external loading and there are a sufficiently large number of transverse cracks in the 90° layers. The entire length of the laminate is L_e and the thickness of cracked layers is H_c. Fig. 4 shows the propagation process of the transverse cracks from state (a) to state (c). In state (a), it is assumed that there exist k uniformly spaced transverse cracks in the laminate. Therefore the crack density in this state is

$$\rho_k = \frac{k}{L_e} \qquad (32)$$

With the changes of external loading, a new transverse crack forms and the crack pattern changes from state (a) to state (b). The number of the transverse cracks increases from k to $(k+1)$. Although in reality a new crack formation is randomly distributed, the overall crack distribution tends to be uniform when the number of cracks is large. In order to simplify the analysis, state (b) is idealized to state (c), in which the $(k+1)$ cracks are also equally spaced. The simplification of the crack spacing here is also due to that the focus of the present study is the effect of crack density on degradation of material properties. The crack density of state (c) is then

$$\rho_{k+1} = \frac{k+1}{L_e} \qquad (33)$$

During the transverse cracking process, the crack surface area increment is H_c. The energy release rate from state (a) to state (b) is

13

$$G = \frac{d\Gamma}{dA}$$

$$= \frac{\Gamma(\rho_{k+1}) - \Gamma(\rho_k)}{H_c} = \frac{(k+1)\Gamma_r(\rho_{k+1}) - k\Gamma_r(\rho_k)}{H_c} \tag{34}$$

$$= \frac{L_e \rho_{k+1} \Gamma_r(\rho_{k+1}) - L_e \rho_k \Gamma_r(\rho_k)}{H_c}$$

where $\Gamma(\rho_{k+1})$ and $\Gamma(\rho_k)$ are the total complementary potential energies of the entire laminate at crack densities ρ_{k+1} and ρ_k, respectively; $\Gamma_r(\rho_{k+1})$ and $\Gamma_r(\rho_k)$ are the respective total complementary potential energies of the representative volume element at crack densities ρ_{k+1} and ρ_k.

The transverse crack propagation criterion

A new crack will form if the energy released due to crack formation reaches the critical energy release rate G_c, i.e.

$$G \geq G_c \tag{35}$$

G_c is a material property and has units of energy per unit area. It can be measured by an experimental method.

Fig. 5 is a flowchart showing how to determine the critical cracking load for a given crack density. For a given load, stress analysis is carried out by using the state space model. The energy release rate G of a representative volume element is then computed by Eq. (34) and compared with G_c. If $G > G_c$, the current load is reduced to achieve a smaller energy release rate until $G = G_c$. If $G < G_c$, the current load is increased to obtain a larger energy release rate until $G = G_c$. If $G = G_c$, the current load is taken as the critical cracking load for the given crack density.

Numerical results

The formulations and criterion proposed above are applied to predict transverse cracking in composite laminates with different configurations, including symmetric cross-ply laminates, symmetric angle-ply laminates and general non-symmetric laminates. The material properties and dimension of these laminates (Liu and Nairn, 1992; Joffe *et al.*, 2001) are given in Table 1. Effects of residual thermal stresses are included in the analysis. ΔT is the difference between the room temperature and the cure temperature. Table 1 also lists the critical energy release rate G_c for each material.

Symmetric laminates subjected to tension

The crack density as a function of applied average stresses for symmetric cross-ply laminates is plotted in Fig.6. Herein, the applied average stress is the axial tension per unit length in the x direction divided by the height H of the laminate. The test and variational results of Liu and Narin (1992) are also shown in these figures for comparisons. The numerical results for Material 1 with $[0°_2/90°_2]_s$ and $[0°_2/90°_4]_s$ lamination profiles are plotted in Figs. 6a and 6b, respectively. Using a single value of G_c, the predictions of the two laminates agree well with the experimental results, which indicates that the critical energy release rate can be used as a material property that characterizes transverse crack propagation in composite materials.

The dependence of crack density on the applied average stress for symmetric angle-ply laminates with layups $[\pm\theta°/90°_4]_s$ are presented in Figs. 7a and 7b. The laminates are composed of Material 2. The present results are compared with those obtained by Monte-Carlo simulations and experimental data in Joffe et al. (2001). Once again very good agreements are observed in these figures. It can be seen that cracks occur earlier in the $[\pm30°/90°_4]_s$ than in the $[\pm15°/90°_4]_s$ laminates.

Non-symmetric laminates subjected to tension

After successful validation for cross-ply symmetric laminates, the method is applied to predict transverse crack propagation in two non-symmetric laminates. The first one is constructed by replacing one set of $90°_4$ layers in the above $[\pm30°/90°_4]_s$ laminate with $0°_4$ layers. Thus the new profile, $[\pm30°/90°_4/0°_4/\mp30°]$, is now non-symmetric. The stress-crack density relation of the non-symmetric laminate is plotted in Fig. 8a. In comparison with Fig. 7b, the onset crack stress of the non-symmetric laminate is significantly increased. The second laminate has a lay-up of $[30°/90°/30°/90°]$ and is composed of Material 3. Both the 90° layers are assumed to have transverse cracks and the crack distributions in both layers are identical. Fig. 8b shows the crack density as a function of the applied average stress in the laminate.

No comparisons have been made in Figs (8a) and (8b), because the present solutions are believed to be the first ones in the literature on predicting transverse crack propagation in non-symmetric laminates. These results, therefore, can be used as benchmarks for testing new models.

Laminates subjected to tension and shearing

In this section, the present method is further used to study the effects of shearing on transverse cracking. A symmetric and a non-symmetric cracked laminates under a combination of tension and shearing are analyzed, respectively. It is assumed that the laminates are composed of Material 3 from Table 1. A series of curves are shown in Fig.9 to demonstrate the effects of shear stresses on the transverse cracking process of a symmetric [30°/90°/90°/30°] laminate. The laminate is subjected to a combined action of uniform tension and shearing. The applied average stress, which is the average stress on the cross-section perpendicular to the *x* axis (Fig 2), increases, while the shear stress keeps constant. The applied shear stresses are -100, -50, 0, 50 and 100 MPa, respectively. It can be seen that both the magnitude and the direction of shear stresses have significant effect on the initiation and development of transverse cracks. The negative shear stresses advance and the positive stresses delay the transverse cracking. This is because the [30°/90°/90°/30°] laminate has a negative shear strain in the x-y plane when the laminate is subjected to a single tension in the *x* direction (Fig 2). If a negative shear stress is also applied, the magnitude of the negative shear strain increases. On the contrary, applying a positive shear stress decreases the magnitude of the shear strain. As a result, the energy release rate in the case of applying negative shear stress is higher than that in the cases of applying no shear stress or positive stresses.

The same set of shear stresses are also applied on a non-symmetric [30°/90°/30°/90°] laminate and the obtained stress-crack density relations are shown in Fig. 10. As can be seen, the effect of shearing on cracking is similar to the symmetric case. Nevertheless, under the same loading condition the crack initiation stress of the non-symmetric laminate is slightly higher than that of the symmetric one. This is because the 90° layers in the symmetric laminate are thicker and a thicker 90° layer is more prone to crack formation.

To the authors' best knowledge, comparable solutions to the results presented in Figs. 9 and 10 are not available in the literature. The results can again be used as benchmark solutions for future development of new theories.

Concluding remarks

16

By using the energy method, an approach based on the state space stress analysis to predict the propagation of transverse cracking in general composite laminates has been proposed. The proposed method inherits the advantages of the state space method, by which an accurate stress distribution and, hence, an accurate estimate of strain energy can be computed. The method can also deal with both symmetric and non-symmetric laminates.

In conjunction with the stress analysis, the energy release rate due to transverse cracking was derived in a laminate with an idealized uniform crack distribution. A new crack forms when the energy release rate approaches the critical energy release rate.

Numerical results for symmetric laminates were compared with alternative numerical solutions and experimental results. The solution was extended to the analysis of non-symmetric laminates under tension, and then to the analysis of general laminates subjected to both tension and shearing. This provided new numerical solutions that are hardly found in the literature. From the new results, it was found that shearing had significant effect on the cracking process.

It is noted that in this work the transverse cracking process was simplified as a crack density increment in a uniformly spaced state, while the nature of the crack multiplication in reality is stochastic. Though good comparisons with test results have been observed for the globe relationship between the applied stresses and crack density, a statistical approach should be resorted to modeling transverse cracking in future work in order to gain deeper understanding of the cracking process.

References

Bailey J E and Parvizi A 1981 On fiber debonding effects and the mechanism of tranverse-ply failure in cross-ply laminates of glass fiber/thermoset composites *Journal of Materials Science* 16 649-59

Dvorak G J and Laws N 1987 Analysis of progressive matrix cracking in composite laminates. II. First ply failure *Journal of Composite Materials* **21** 309-29

Fan J and Zhang J 1993 In-situ damage evolution and micro/macro transition for laminated composites *Composites Science and Technology* **47** 107

Flaggs D L 1985 Prediction of tensile matrix failure in composite laminates *Journal of Composite Materials* **19** 29

Flaggs D L and Kural M H 1982 Experimental determination of the in situ transverse lamina strength in graphite/epoxy laminates *Journal of Composite Materials* **16** 103-16

Garrett K W and Bailey J E 1977 Multiple transverse fracture in 90°; cross-ply laminates of a glass fibre-reinforced polyester *Journal of Materials Science* **12** 157

Herakovich, C.T., 1998. Mechanics of fibrous composites. Wiley, New York.

Joffe R, Krasnikovs A and Varna J 2001 COD-based simulation of transverse cracking and stiffness reduction in $[\theta/90_n]_s$ laminates *Composites Science and Technology* **61** 637-56

Laws N and Dvorak G J 1988 Progressive transverse cracking in composite laminates *Journal of Composite Materials* **22** 900-16

Leblond P, El Mahi A and Berthelot J M 1996 2D and 3D numerical models of transverse cracking in cross-ply laminates *Composites Science and Technology* **56** 793

Lim S-H and Li S 2005 Energy release rates for transverse cracking and delaminations induced by transverse cracks in laminated composites *Composites Part A (Applied Science and Manufacturing)* **36** 1467-7

Liu S and Nairn J A 1992 The formation and propagation of matrix microcracks in cross-ply laminates during static loading *Journal of Reinforced Plastics and Composites* **11** 158-78

McCartney L N 1998 Predicting transverse crack formation in cross-ply laminates *Composites Science and Technology* **58** 1069-81

McCartney L N 2000 Model to predict effects of triaxial loading on ply cracking in general symmetric laminates *Composites Science and Technology* **60** 2255

McCartney L N 2004 Effect of mixed mode loading on ply crack development in laminated composites: theory and application. Nat. Phys. Lab., Teddington, UK) p iv+22

McCartney L N 2005 Energy-based prediction of progressive ply cracking and strength of general symmetric laminates using an homogenisation method *Composites Part A (Applied Science and Manufacturing)* **36** 119-28

Nairn J A 1989 The strain energy release rate of composite microcracking: a variational approach *Journal of Composite Materials* **23** 1106

Nairn J A 2000 *Comprehensive Composite Materials,* ed Z Anthony Kelly and Carl (Oxford: Pergamon) p 403

Nairn J A and Hu S 1992 The formation and effect of outer-ply microcracks in cross-ply laminates: a variational approach *Engineering Fracture Mechanics* **41** 203-21

Nairn J A, Hu S and Bark J S 1993 A critical evaluation of theories for predicting microcracking in composite laminates *Journal of Materials Science* **28** 5099-111

Parvizi A, Garrett K W and Bailey J E 1978 Constrained cracking in glass fibre-reinforced epoxy cross-ply laminates *Journal of Materials Science* **13** 195-201

Sirivedin S, Fenner D N, Nath R B and Galiotis C 2006 Viscoplastic finite element analysis of matrix crack propagation in model continuous-carbon fibre/epoxy composites *Composites Part A: Applied Science and Manufacturing* **37** 1922-35

Smith P A and Ogin S L 1999 On transverse matrix cracking in cross-ply laminates loaded in simple bending *Composites - Part A: Applied Science and Manufacturing* **30** 1003.

Soldatos, K.P. and Ye, J.Q. (1994). Wave propagation in anisotropic laminated hollow cylinders of infinite extent. *Journal of Acoustics Society of America.* **96**(5), Part I, 3744-3752.

Wang A S D, Kishore N N and Li C A 1985 Crack development in graphite-epoxy cross-ply laminates under uniaxial tension *Composites Science and Technology* **24** 1

Ye J Q 2002 *Laminated Composite Plates and shells: 3D Modelling* (London: Springer)

Ye J Q and Sheng H Y 2003 Free-edge effect in cross-ply laminated hollow cylinders subjected to axisymmetric transverse loads *International Journal of Mechanical Sciences* **45** 1309-26

Ye J Q, Sheng H Y and Qin Q H 2004 A state space finite element for laminated composites with free edges and subjected to transverse and in-plane loads. *Computers and Structures* **82**(15/16) 1131-1141.

Ye J Q and Soldatos K P 1994a Three-dimensional stress analysis of orthotropic and cross-ply laminated hollow cylinders and cylindrical panels *Computer Methods in Applied Mechanics and Engineering* **117** 331-51

Ye J Q and Soldatos K P 1994b Three-dimensional vibration of laminated cylinders and cylindrical panels with symmetric or antisymmetric cross-ply lay-up *Composites Engineering* **4** 429-44

Ye J Q and Soldatos K P 1995 Three-dimensional buckling analysis of laminated composite hollow cylinders and cylindrical panels *International Journal of Solids and Structures* **32** 1949-62

Ye J Q and Soldatos K P 1996 Three-dimensional vibration of laminated composite plates and cylindrical panels with arbitrarily located lateral surfaces point supports *International Journal of Mechanical Sciences* **38** 271-81

Yokozeki T, Aoki T and Ishikawa T 2002 Transverse crack propagation in the specimen width direction of CFRP laminates under static tensile loadings *Journal of Composite Materials* **36** 2085

Yokozeki T, Aoki T and Ishikawa T 2005 Consecutive matrix cracking in contiguous plies of composite laminates *International Journal of Solids and Structures* **42** 2785

Zhang J, Fan J and Soutis C 1992 Analysis of multiple matrix cracking in $[\pm\theta_m/90_n]_s$ composite laminates. 1. In-plane stiffness properties *Composites* **23** 291.

Zhang D, Ye J Q and Lam D 2007a Free-edge and Ply Cracking Effect in Angle-ply Laminated Composites subjected to In-plane Loads *Journal of Engineering Mechanics, Transactions ASCE* **133**(12) 1268-1277.

Zhang D, Ye J Q and Lam D 2007b Properties degradation induced by transverse cracks in general symmetric laminates *International Journal of Solids and Structure* **44**(17) 5499-5517.

Table 1 Material properties and dimensions

	Material 1	Material 2	Material 3
Type	Fiberite 934/T300	Glass/epoxy	Graphite/epoxy
E_L	128 GPa	44.73 GPa	144.78 GPa
E_T	7.2 GPa	12.76 GPa	9.58 GPa
ν_{LT}	0.3	0.297	0.31
ν_{TT}	0.5	0.42	0.52
G_{LT}	4.0 GPa	5.8 GPa	4.97 GPa
G_{TT}	2.4 GPa	4.49 GPa	3.37 GPa
α_1	$-0.09\times10^{-6}/^oC$	$8.6\times10^{-6}/^oC$	*N/A*
α_2	$28.8\times10^{-6}/^oC$	$22.1\times10^{-6}/^oC$	*N/A*
ΔT	$-125\ ^oC$	$-105\ ^oC$	0^oC
G_c	690 J/m^2	610 J/m^2	900 J/m^2
L_e	50 mm	50 mm	50 mm
H_{ply}	0.154 mm	0.144 mm	0.127 mm
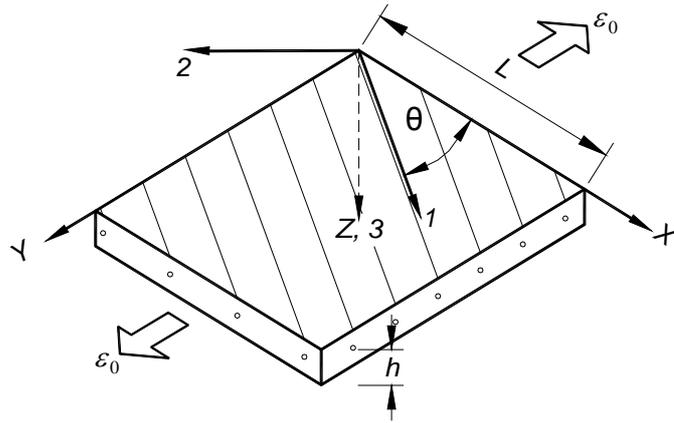
Fig. 1 Nomenclature of an off-axis lamina.
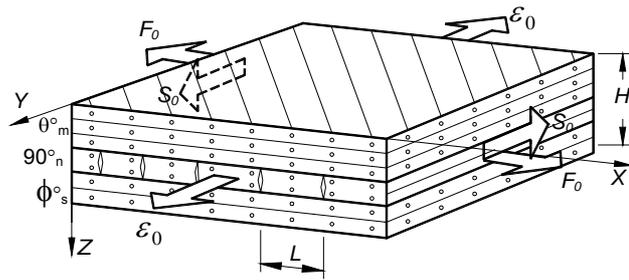
Fig. 2 Schematic view of a $[\theta^\circ_m/90^\circ_n/\phi^\circ_s]$ laminate with an array of transverse ply cracks in 90°_n layers.
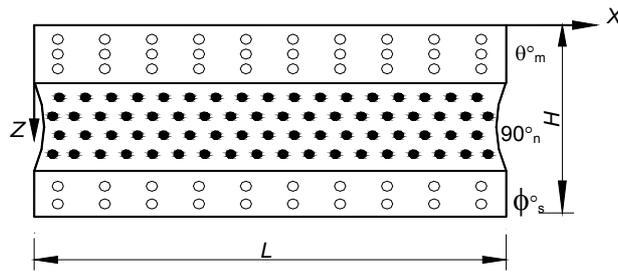
Fig. 3 A representative volume element of a $[\theta^\circ_m/90^\circ_n/\phi^\circ_s]$ laminate with ply cracks in 90°_n layers.
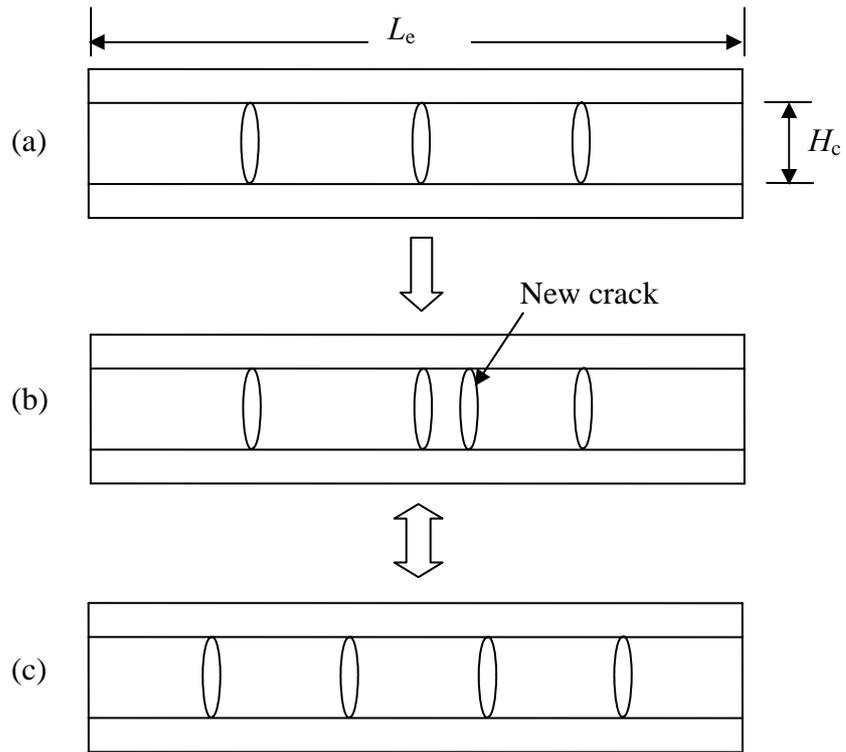
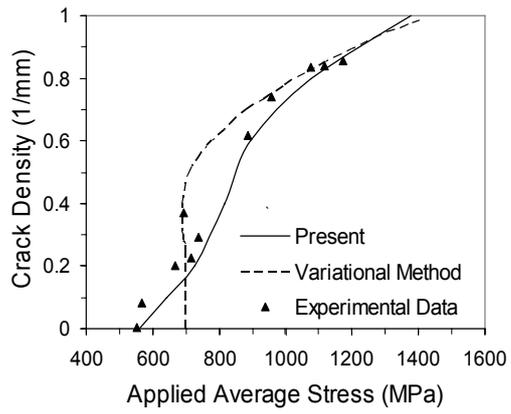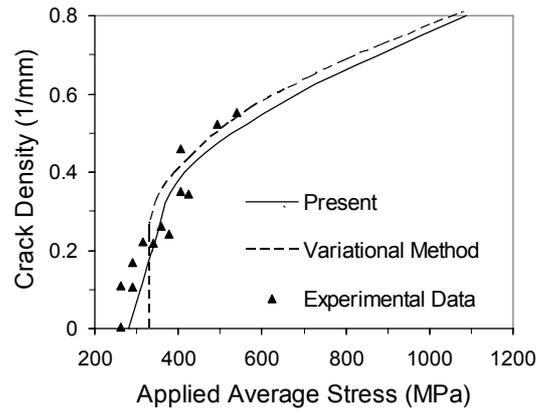Fig. 4 Nomenclature of the propagation process of transverse cracks and the idealised uniform distribution state.
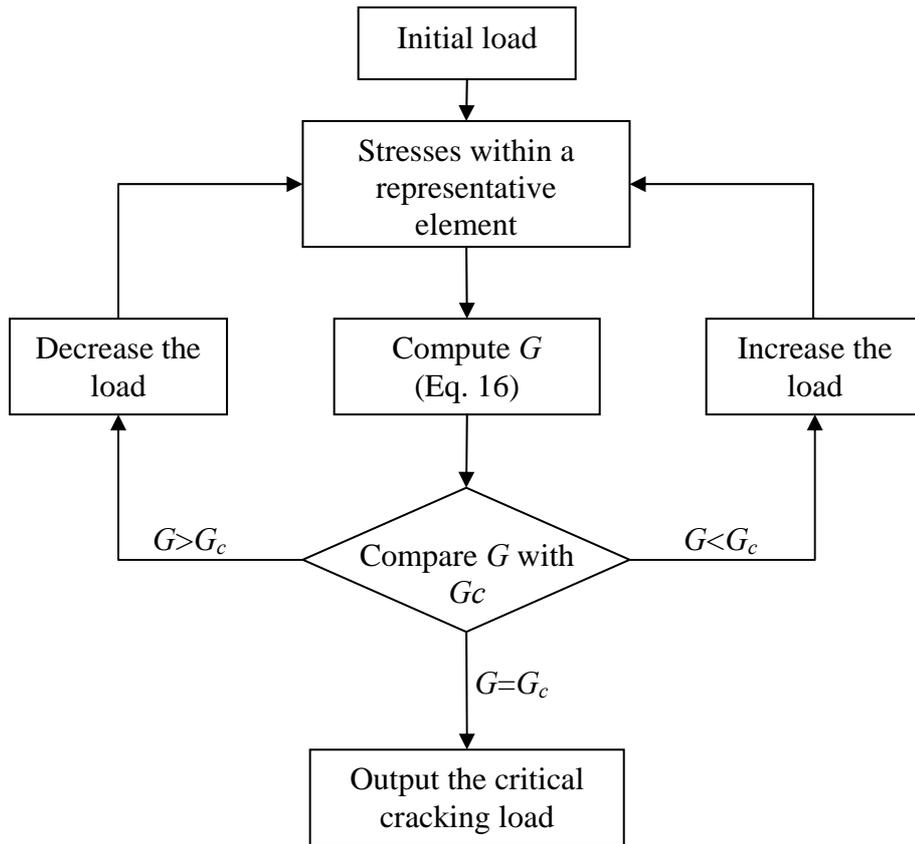
Fig. 5. Flowchart of calculating critical cracking load for a given crack density.

Fig. 6 Dependence of crack density on the applied average stress in
(a) Fiberite 934/T300 $[0°_2/90°_2]_s$ laminate with transverse cracks.
(b) Fiberite 934/T300 $[0°_2/90°_4]_s$ laminate with transverse cracks
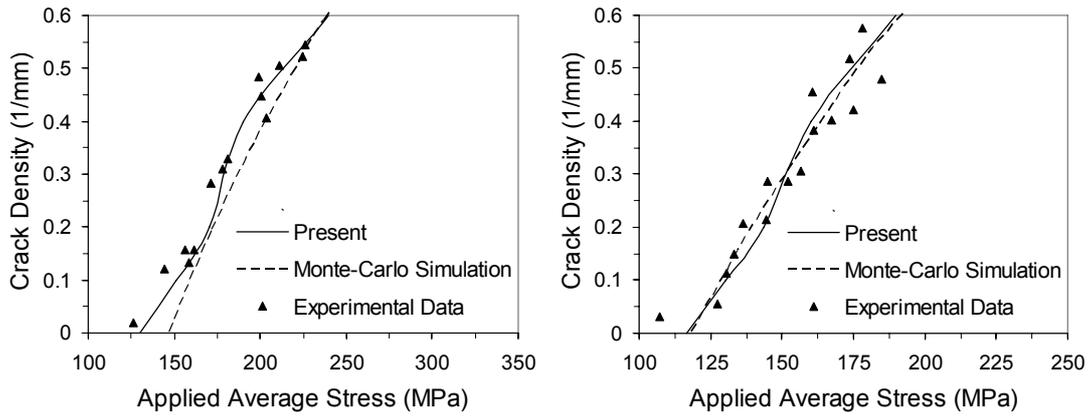
Fig. 7 Dependence of crack density on the applied average stress in
(a) $[\pm 15°/90°_4]_s$ glass/epoxy laminate with transverse cracks.
(b) $[\pm 30°/90°_4]_s$ glass/epoxy laminate with transverse cracks.
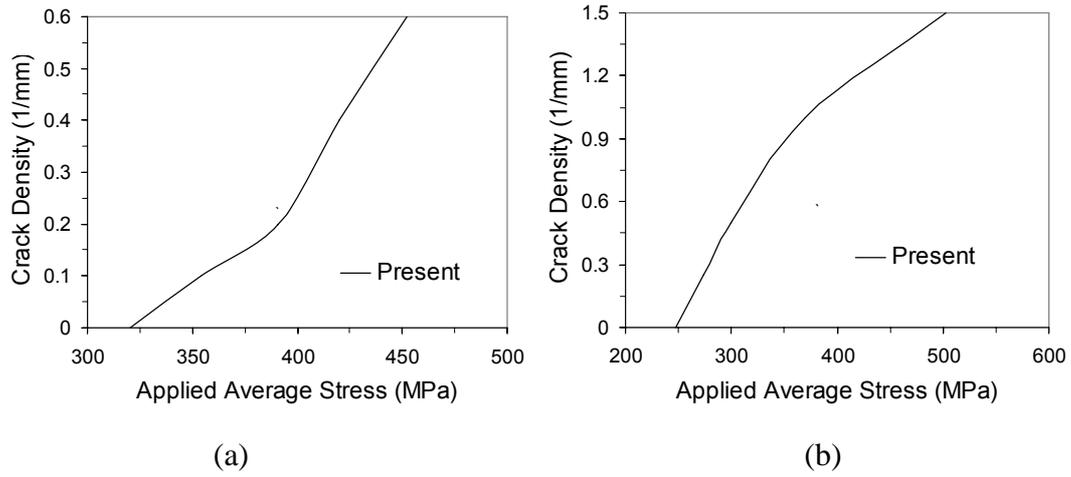
Fig. 8. Dependence of crack density on the applied average stress in
(a) $[\pm 30°/90°_4/0°_4/\mp 30°]$ glass/epoxy laminate with transverse cracks;
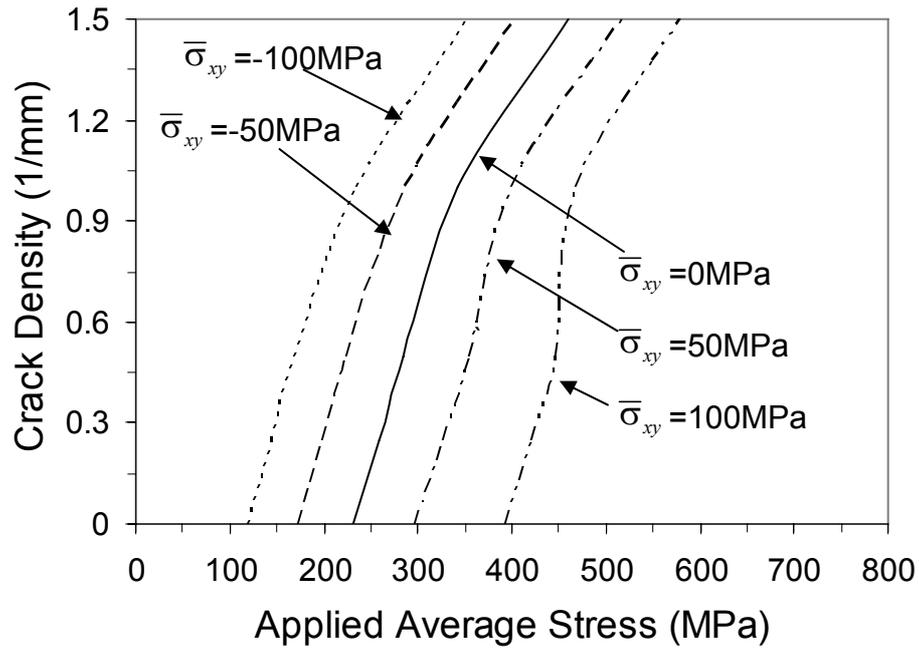(b) $[30°/90°/30°/90°]$ graphite/epoxy laminate with transverse cracks.

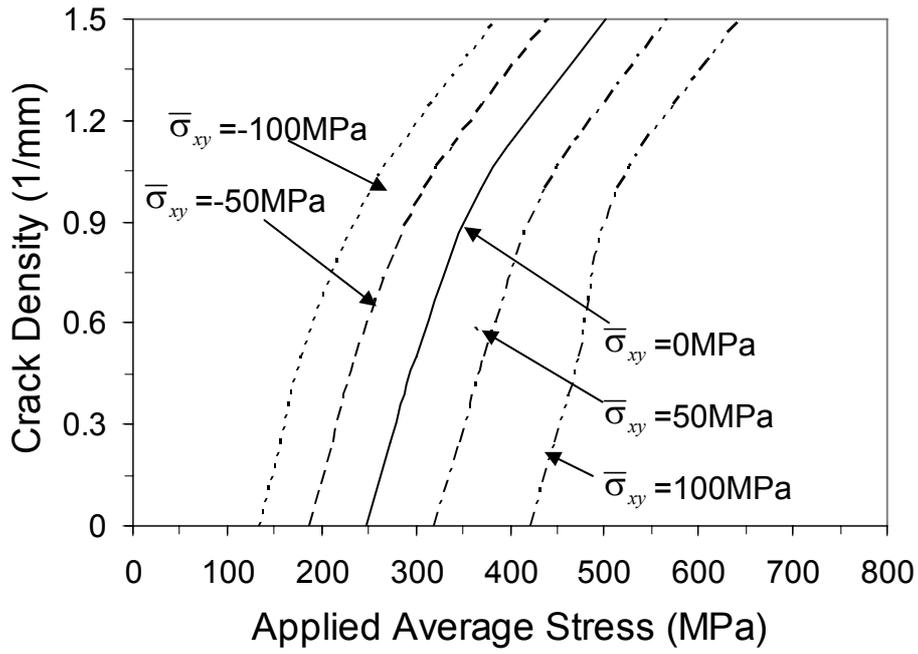Fig.9. Dependence of crack density on the applied average stress and shear stresses in a [30°/90°/90°/30°] graphite/epoxy laminate.

Fig.10. Dependence of crack density on the applied average stress and shear stresses in a [30°/90°/30°/90°] graphite/epoxy laminate.